IEEE Access
Multidisciplinary | Rapid Review | Open Access Journal

Received January 18, 2020, accepted February 7, 2020, date of publication February 19, 2020, date of current version March 2, 2020.

Digital Object Identifier 10.1109/ACCESS.2020.2975008

Multi-Agent Trajectory-Tracking Flexible Formation via Generalized Flocking and Leader-Average Sliding Mode Control

JUN ZHOU, (Member, IEEE), DEBIN ZENG, AND XINBIAO LU
Department of Control Engineering, School of Energy and Electrical Engineering, Hohai University, Nanjing 211100, China
Corresponding author: Jun Zhou (jzhouaguar@163.com)

This work was supported by the National Nature Science Foundation of China under Grant 61573001.

ABSTRACT This paper reports a flexible (or time-varying) multi-agent formation approach with average trajectory tracking for second-order integral multi-agent networks with single virtual leaders. The approach is developed by means of time-varying Olfati-Saber flocking algorithms, and sliding mode control (SMC) in terms of the leader-average dynamics. More precisely, SMC-specifying average trajectory tracking is combined with flexible multi-agent flocking driven by the Olfati-Saber flocking algorithms with time-varying weighting norm. Existence conditions and properties of the suggested multi-agent formation are examined rigorously, together with implementation formulas. It is shown that by designing the sliding surface and the time-varying weighting matrix appropriately, flexible formation with finite-time trajectory tracking can be achieved, free of control action chattering; moreover, the sliding mode control and formation control can be designed separately. Numerical examples are given to illustrate the main results.

INDEX TERMS Multi-agent, flexible flocking formation, leader-average model, sliding mode control, trajectory tracking.

I. INTRODUCTION

Miscellaneous systems can be modeled as multi-agent networks, while various control problems can be reformulated as formation manipulation of the dynamics and behaviours of the multi-agent networks. In the literature, multi-agent control theory and applications have been attacked intensively, for example in [18], [30], [38], [42], [43], [45], [46], [49], [55], [57]. In the latest score of years, fruitful results and numerous expansions on multi-agent control are reported, in which the controlled plants are modeled as self-driven [7], [22], sampled-data [13], [17], time-delayed and nonlinear ones with or without uncertainties/disturbances [5], [19], [21], [32], [54]. As real world applications, multi-agent flocking strategies are adopted in autonomous unmanned vehicles as in [16], [48]; multi-agent collision control is exploited for power swing reduction and frequency synchronism in large-scale power systems [51], [60].

Formation control in networked systems is an inevitable task in geographic data scanning, military surveillance, and robots routing and task cooperating. As a matter of fact, there are numerous papers related to formation control, regarding various types of networked plants [3], [7], [8], [11], [14], [23]–[25], [33]–[35], [40], [41], [47], [52], [53], [58]. Formation control with targeting and/or trajectory tracking is discussed in [26]. Eigen-structure assignment in formation control is considered by [29]. Formation control with multi-agent orientation rolling and shaping is examined by [20], [39]. Formation control under iterative learning can be found in [4], [27], [28]. To achieve flexible or time-varying multi-agent formation, interesting discussions are summarized in [1], [9], [10], [15], [50].

In this study, the generalized flocking algorithms of [31], [59] for the second-order integral multi-agent networks with single virtual leaders are further extended by employing time-varying weighting matrices in position and velocity metrics for flexible multi-agent formation control. As the main results, existence and properties about the flexible formation aspect under the suggested algorithms are summarized. To address the trajectory-tracking aspect, the navigation features of the leader-average dynamics are exploited. More specifically, based on the sliding mode control techniques [6], [12], [36], [37], [44], [56], [61], the transient/steady-state average dynamics are manipulated for

The associate editor coordinating the review of this manuscript and approving it for publication was Jiahu Qin.

the leader-average state to slide on the sliding surface specified along the tracked trajectory, while the flexible formation is retained simultaneously. Advantages of the approach include: (a) the control algorithms for flexible formation and sliding mode can be designed separately; (b) the sliding mode control for navigation keeps the trajectory tracking from matched noise, while the average trajectory-tracking is attainable in finite time; (c) the sliding mode is virtual, and no chattering control actions are practically involved.

Outlines: Preliminaries to second-order integral multi-agent networks are collected in Section II. Section III explicates the flocking algorithms with time-varying weighting parameters. Leader-average modeling and sliding mode control are explicated in Section IV. Trajectory-tracking formation control is formulated and addressed in Section V with respect to the leader-average model. Illustrations are sketched in Section VI, and Section VII is our conclusion.

Notations: $\mathcal{R}$ and $\mathcal{C}$ denote the sets of all real and complex numbers, respectively. I_n denotes the $n \times n$ identity matrix. $(\cdot) \otimes (*)$ means the Kronecker product of the matrices $(\cdot)$ and $(*)$. $|\cdot|$ means the absolute value of a scalar complex number, the Euclidean vector norm and the induced matrix norm as appropriately according to the context.

II. PRELIMINARIES TO MULTI-AGENT NETWORKS

Firstly, let us consider a multi-agent network consisting of N agents, each of which is described by the second-order continuous-time state-space equation

$$\dot{q}_i(t) = p_i(t), \quad \dot{p}_i(t) = u_i(t), \ t \geq 0 \tag{1}$$

with $i \in \{1, \cdots, N\} := \mathcal{N}$. In (1), $q_i(t), p_i(t), u_i(t) \in \mathcal{R}^n$ are the position, velocity and acceleration vectors, respectively, of the agent i at time t. Throughout the paper, we write $\dot{(\cdot)} = d(\cdot)/dt$. The time variable t will be dropped.

For our latter usage, let us define the vectorization of $\{q_i\}_{i=1}^N$, $\{p_i\}_{i=1}^N$ and $\{u_i\}_{i=1}^N$, respectively, as follows.

$$\begin{cases} q =: vec\{q_i\} = [q_1^T, q_2^T, \cdots, q_N^T]^T \in \mathcal{R}^{Nn} \\ p =: vec\{p_i\} \in \mathcal{R}^{Nn}, \quad u =: vec\{u_i\} \in \mathcal{R}^{Nn} \end{cases}$$

Accordingly, the multi-agent network with the agents individually defined by (1) can be re-written collectively as the (Nn)-dimensional model (2).

$$\dot{q} = p, \quad \dot{p} = u, \ t \geq 0 \tag{2}$$

Secondly, let $M_t =: M(t) \in \mathcal{R}^{n\times n}$ be a time-varying weighting matrix for inter-agent position difference metric in the Euclidean norm sense of

$$|M_t \Delta q_{ij}| = |M_t(q_i - q_j)|$$

Based on this, the γ-neighbor of the agent i is defined as

$$\mathcal{N}_{i,t} =: \{j \in \mathcal{N} : \text{if } |M_t \Delta q_{ij}| < \gamma\}$$

where $\gamma > 0$ is the radius of the super-ball in $\mathcal{R}^n$; $\mathcal{N}_{i,t} \subseteq \mathcal{N}$ for all $t \geq 0$. By the definition, $\mathcal{N}_{i,t}$ is the subscript set of all agents in the neighborhood of the agent i at t. The same radius is meant in all neighborhoods.

Thirdly, let $(i \times j)$ be an undirected connection between the agents i and j if both are in each other's γ-neighborhood, and thus their position and velocity data are available mutually. The graph of the multi-agent network at t is

$$\mathcal{G}_t = \{(i \times j) : j \in \mathcal{N}_{i,t}, i \neq j, \forall\, i \in \mathcal{N}\} \subset \mathcal{N} \times \mathcal{N} \tag{3}$$

That is, for each specific $t \in [0, \infty)$, $\mathcal{G}_t$ is a subgraph of $\mathcal{N} \times \mathcal{N} = \{(i \times j) : \forall\, i, j \in \mathcal{N}, i \neq j\}$, which is a set of all one-to-one connections in the multi-agent network.

III. FLEXIBLE MULTI-AGENT FORMATION CONTROL

Now we formulate the formation control: fix the control actions $\{u_i\}_{i=1}^N$ such that distributed and localized feedbacks are built and the following relationships hold.

$$\begin{cases} 0 < |M_t \Delta q_{ij}| < \gamma, & \forall\, (i \times j) \in \mathcal{G}_t, \ i \neq j, \\ & \forall\, t \in [0, \infty) \\ \lim\limits_{t\to\infty} |M_t \Delta q_{ij}| = d, & \forall\, (i \times j) \in \mathcal{G}_\infty, \ i \neq j, \\ & 0 < d < \gamma \\ \lim\limits_{t\to\infty} p_i = p^*, & \forall\, i \in \mathcal{N}, \ \exists p^* \neq 0 \in \mathcal{R}^n \\ M_t \not\equiv 0, & \forall t \in [0, \infty) \end{cases} \tag{4}$$

where $\mathcal{G}_\infty$ is the graph of the multi-agent network at $t \to \infty$. In (4), the first relation reflects the agent behavior rules: neither collision nor splitting all the time; the second and third relations are to achieve the specified formation and velocity consensus in the steady-state. $M_t \neq 0$ and $0 < d < \gamma$ are assumed for the γ-neighborhood and the limit to be well-defined. Also, $p^* \neq 0$ ensures that velocity consensus is rigorously meant in orientation and magnitude.

A. TIME-VARYING FLOCKING CONTROL

Build the time-varying generalized Olfati-Saber algorithm based on [31], [59] as follows.

$$\begin{aligned} u_i = & -\Sigma_{j\in\mathcal{N}_{i,t}} \phi(M_t(q_j - q_i)) M_t^T n_{ij}(M_t(q_i - q_j)) \\ & - \Sigma_{j\in\mathcal{N}_{i,t}} a_{ij}(M_t(q_j - q_i)) M_t^T M_t(p_i - p_j) \\ & - [\Phi^T \Phi(q_i - q_r) + \Psi(p_i - p_r)] \end{aligned} \tag{5}$$

where $\Phi \in \mathcal{R}^{n\times n}$ is non-singular and $0 < \Psi^T = \Psi \in \mathcal{R}^{n\times n}$. The control action u_i defined by (5) is determined by the time-varying flocking control algorithm.

To explicate the algorithm, we write $z =: q_j - q_i$. About the first term in (5), we use the following notations.

$$\phi(M_t z) =: \frac{\rho(|M_t z|_\sigma / \gamma_\sigma, \eta)}{2} \cdot \Big[\frac{(|M_t z|_\sigma - d_\sigma + c)(a+b)}{\sqrt{1 + (|M_t z|_\sigma - d_\sigma + c)^2}} + (a - b)\Big]$$

where a, b, c satisfy $0 < a \leq b$ and $c = |a - b|/\sqrt{4ab} > 0$. $d_\sigma = |d|_\sigma = \epsilon^{-1}[\sqrt{1 + \epsilon d^2} - 1]$ and $\gamma_\sigma = |\gamma|_\sigma = \epsilon^{-1}[\sqrt{1 + \epsilon\gamma^2} - 1]$. Since $0 < d < \gamma$, it

holds that $0 < d_\sigma < \gamma_\sigma$. Here, $|\cdot|_\sigma$ is called the σ-norm

$$|M_t z|_\sigma = \epsilon^{-1}\Big(\sqrt{1+\epsilon|M_t z|^2}-1\Big) : \mathcal{R}^n \to \mathcal{R}_0^+$$

where $\epsilon > 0$ is a parameter and $\mathcal{R}_0^+ = \{s \in \mathcal{R} : s \geq 0\}$.

The bump function $\rho(\cdot,\cdot)$ is a scalar mapping given by

$$\rho(|M_t z|_\sigma/\gamma_\sigma, \eta) = \begin{cases} 1, & |M_t z|_\sigma/\gamma_\sigma \in [0,\eta) \\ \frac{1}{2}[1+\cos(\pi \cdot \frac{|M_t z|_\sigma/\gamma_\sigma - \eta}{1-\eta})], \\ \qquad |M_t z|_\sigma/\gamma_\sigma \in [\eta, 1] \\ 0, & \text{otherwise} \end{cases}$$

with $\eta \in (0,1)$. For fixed η, $\rho(z,\eta) \in [0,1]$ is C^1-smooth, and $\partial\rho(z,\eta)/\partial z = 0$ over $z \in [1,\infty)$.

Also about the first term of (5), for all $i, j \in \mathcal{N}$, we have

$$\begin{cases} n_{ij}(M_t(-z)) = \dfrac{-M_t z}{\sqrt{1+\epsilon|M_t z|^2}} = -n_{ji}(M_t z) \in \mathcal{R}^n \\ \varphi(M_t z) =: \displaystyle\int_{d_\sigma}^{|M_t z|_\sigma} \phi(s)ds \end{cases}$$

To see the second term of (5), define the adjacent function

$$a_{ij}(M_t(q_j - q_i)) =: \begin{cases} 0, & \forall\, i = j, \quad or\ j \notin \mathcal{N}_{i,t} \\ \rho(|M_t(q_j-q_i)|_\sigma/\gamma_\sigma, \eta), \\ \qquad \forall\, i \neq j,\ j \in \mathcal{N}_{i,t} \end{cases} \tag{6}$$

In what follows, we call

$$A(\mathbf{M}_t q) =: \{a_{ij}(M_t(q_j - q_i))\} \in \mathcal{R}^{N\times N}$$

the spatial adjacency matrix for the position vectorization q. Here, $\mathbf{M}_t = I_N \otimes M_t \in \mathcal{R}^{Nn\times Nn}$. Clearly, $A(\mathbf{M}_t q)$ is symmetrical with non-negative entries, whose scalar Laplacian matrix and the multi-dimensional Laplacian matrix, denoted by $L(\mathbf{M}_t q)$ and $\mathbf{L}(\mathbf{M}_t q)$, are given by

$$\begin{cases} L(\mathbf{M}_t q) = \Delta A(\mathbf{M}_t q) - A(\mathbf{M}_t q) \in \mathcal{R}^{N\times N} \\ \mathbf{L}(\mathbf{M}_t q) = L(\mathbf{M}_t q) \otimes I_n \in \mathcal{R}^{Nn\times Nn} \end{cases} \tag{7}$$

where $\Delta(\cdot)$ is the degree matrix of $(\cdot)$. Its diagonal entries are the row-sums of $(\cdot)$ and non-diagonal ones are zeros.

To understand the third term of (5), we need the virtual leader agent model

$$\dot{q}_r = p_r, \quad \dot{p}_r = u_r, \quad t \geq 0 \tag{8}$$

with $q_r, p_r \in \mathcal{R}^n$. The leader agent provides navigation such that additional objectives for the agents to track the leader behavior and so on can be taken into account.

Remark 1: Since the leader is virtual, no leader agent exists such that q_r and p_r are measured and informed to all the agents. When implementing the protocol in the follower agents, the leader agent is nothing but a navigation program driven by q_a and p_a, which are the average position and velocity that can be obtained by distributed measurements and data exchanges in between the agents.

B. AVERAGE MODELING

To see existence and properties under the time-varying flocking algorithm (5), we explain the average model for the closed-loop multi-agent dynamics. Define the average position and velocity vectors, respectively, by

$$q_a = N^{-1}\Sigma_{i=1}^N q_i, \quad p_a = N^{-1}\Sigma_{i=1}^N p_i$$

Accordingly, by summing all individual equations in (1) under the time-varying flocking algorithms (5) and multiplying the sum equation with $1/N$, it follows that

$$\dot{q}_a = p_a, \quad \dot{p}_a = -\Phi^T\Phi(q_a - q_r) - \Psi(p_a - p_r) \tag{9}$$

In deriving (9), we used $\Sigma_{i=1}^N u_{1,i} = 0$ and $\Sigma_{i=1}^N u_{2,i} = 0$.

Thirdly, let us introduce new position and velocity vectors with respect to the average frame (q_a, p_a); that is

$$x_i = q_i - q_a, \quad v_i = p_i - p_a$$

Correspondingly, $x_j - x_i = q_j - q_i$ and $v_j - v_i = p_j - p_i$ hold true. If we further define

$$x =: \text{vec}\{x_i\} \in \mathcal{R}^{Nn}, \quad v =: \text{vec}\{v_i\} \in \mathcal{R}^{Nn}$$

Eventually, the closed-loop multi-agent dynamics can be reflected under the shifting frame (x, v) by the structural dynamics model

$$\begin{cases} \dot{x} = v, \\ \dot{v} = -\mathbf{M}_t^T\mathbf{V}(\mathbf{M}_t x)\mathbf{M}_t x - \mathbf{M}_t^T\mathbf{L}(\mathbf{M}_t x)\mathbf{M}_t v \\ \qquad -[\Phi^T\Phi x + \Psi v] \end{cases} \tag{10}$$

where $\mathbf{V}(\mathbf{M}_t x)$ is similar to $\mathbf{L}(\mathbf{M}_t x)$ but in terms of the Lyapunov functional $V(M_t, x)$ defined according to [59].

The closed-loop multi-agent network (10) is time-varying and highly nonlinear, whose solution cannot be given explicitly. However, fortunately, its Hamiltonian equivalence can help us in proving Theorem 1, though the details are omitted due to space limitation and to avoid redundance.

C. EXISTENCE AND PROPERTIES OF FLEXIBLE MULTI-AGENT FORMATION

Now we are ready to conclude Theorem 1 about flexible flocking formation under the algorithm (5), which is a time-varying version of Theorem 3.1 [59].

Theorem 1: Consider the multi-agent network with agents individually defined by (1). To each agent, the time-varying flocking algorithm (5) is imposed, in which $M_t \not\equiv 0 \in \mathcal{R}^{n\times n}$, $|M_t| < \kappa$ over $t \geq 0$ for some $0 < \kappa < \infty$ and $M_t^T\dot{M}_t = \dot{M}_t^T M_t \leq 0$ for all $t \geq 0$; in addition, $\Phi \in \mathcal{R}^{n\times n}$ is nonsingular and $0 < \Psi^T = \Psi \in \mathcal{R}^{n\times n}$. Let $K(v) = |v|^2/2$ and $J(\Phi, x) = |\Phi x|^2/2$. If $K(v)|_{t=0} < \infty$ and $J(\Phi, x)|_{t=0} < \infty$, then we have

(i) *The multi-agents remain cohesive along the average trajectory q_a; that is, a radius $0 < \Upsilon < \infty$ uniformly in $t \geq 0$ exists such that $|q - q_a| \leq \Upsilon$ over $t \geq 0$.*

(ii) *$|v(t)| \to 0$ as $t \to \infty$ is always achievable; that is, $\lim_{t\to\infty} p_1 = \cdots = \lim_{t\to\infty} p_N = p^*$ with $p^* = \lim_{t\to\infty} p_a(t) \in \mathcal{R}^{Nn}$.*

(iii) *Almost every solution x to (10) asymptotically converges to an equilibrium, where $V(M_t, x) + J(\Phi, x)$ is locally minimized.*

(iv) *If $\sup_{t\in[0,\infty)} |M_t|$ is sufficiently small, then multi-agent collision occurs ultimately as $t \to \infty$ in the sense of $\lim_{t\to\infty} |q_i - q_j| = 0$ for all $i, j \in \mathcal{N}$.*

Here, $M_t^T \dot{M}_t = \dot{M}_t^T M_t \leq 0$ over $t \geq 0$ means that $M_t^T \dot{M}_t$ is symmetric and negative semi-definite for each fixed $t \geq 0$.

Remark 2: If M_t is differentiable almost everywhere (that is, it is not differentiable only in a set of measure zero) and $M_t^T \dot{M}_t$ is symmetric, $M_t^T \dot{M}_t = \dot{M}_t^T M_t \leq 0$ is satisfied when one of the following conditions is true.

(A1). M_t is piecewise constant for all $t \geq 0$;

(A2). $\dot{M}_t = -M_t$ for all $t \geq 0$;

(A3). $M_t = \alpha(t)M$, where $M \in \mathcal{R}^{n\times n}$ is a constant matrix and $\alpha(t)$ is a scalar function in t satisfying $\alpha(t)\dot{\alpha}(t) \leq 0$ for all $t \geq 0$.

Remark 3: The assertions (i)-(iii) of Theorem 1 say that if M_t is moderate in the magnitude sense of $|M_t|$, flexible formation almost always exists in the steady state. The assertion (iv) says that multi-agent formation may not happen, if a small-magnitude M_t is adopted so that rejecting forces are not strong enough to keep away from each other.

Remark 4: According to [59], the proof arguments about Theorem 1 are based on the structural dynamic model (10). The model has nothing to do with q_a, p_a, q_r and p_r algebraically. In view of this, we conclude that Theorem 1 holds true no matter what behaviors q_a, p_a, q_r and p_r possess; or flexible formation is achievable independent of q_a, p_a, q_r and p_r. This is the starting point for us to introduce sliding mode control to manipulate q_a, p_a, q_r and p_r, while flexible formation remains unchanged.

IV. LEADER-AVERAGE MODEL AND SLIDING MODE CONTROL

A. LEADER-AVERAGE DYNAMICS AND STRUCTURAL FEATURES

To understand the leader-average dynamics of the closed-loop multi-agent network, let us re-express (8) and (9) with the augmented vector $[q_a^T, p_a^T \,|\, q_r^T, p_r^T]^T \in \mathcal{R}^{4n}$ as follows.

$$\underbrace{\left[\begin{array}{c} \dot{q}_a \\ \dot{p}_a \\ \hline \dot{q}_r \\ \dot{p}_r \end{array}\right]}_{\dot{\xi}} = \underbrace{\left[\begin{array}{ccc|c} 0 & I_n & 0 & 0 \\ -\Phi^T\Phi & -\Psi & \Phi^T\Phi & \Psi \\ 0 & 0 & 0 & I_n \\ \hline 0 & 0 & 0 & 0 \end{array}\right]}_{A} \cdot \underbrace{\left[\begin{array}{c} q_a \\ p_a \\ \hline q_r \\ p_r \end{array}\right]}_{\xi} + \underbrace{\left[\begin{array}{c} 0 \\ 0 \\ \hline 0 \\ I_n \end{array}\right]}_{B} u_r \qquad (11)$$

which is termed the leader-average equation. Clearly, the weighting matrix M_t is not in (11). Also we notice

- Firstly, since (11) is LTI, the multi-agent formation with expected stead-state average features is meant in the sense of $t \to \infty$. Hence to realize finite-time trajectory-tracking formation under the control algorithms (5), the sliding mode control is used.
- Secondly, the controllability matrix for (11) is

$$Q_C(s) =: [\, sI_{4n} - A \,|\quad B\,] \in \mathcal{R}^{4n\times 5n}$$

Since $\Phi^T\Phi > 0$, $\text{rank}\,\{Q_C(s)\} = 4n$ for all $s \in \mathcal{C}$. The PBH criterion says that the leader-average dynamics (11) are controllable if $\Phi^T\Phi > 0$. This in turn implies that by choosing the leader reference u_r appropriately, the multi-agent average trajectories can be specified.

B. SMC IN LEADER-AVERAGE DYNAMICS

In this subsection, we formulate and address leader-average SMC for accommodating flexible formation with finite-time average trajectory tracking.

We re-write the leader-average equation (11) as

$$\left[\begin{array}{c} \dot{\xi}_1 \\ \hline \dot{\xi}_2 \end{array}\right] = \left[\begin{array}{c|c} A_{11} & A_{12} \\ \hline 0 & A_{22} \end{array}\right] \left[\begin{array}{c} \xi_1 \\ \hline \xi_2 \end{array}\right] + \left[\begin{array}{c} 0 \\ \hline I_n \end{array}\right] u_r \qquad (12)$$

By the structural facts, the pairs (A, B) and (A_{11}, A_{12}) are controllable under $\Phi^T\Phi > 0$.

With respect to (12), let us define the switching function $s : \mathcal{R}^{4n} \times \mathcal{R}^n \to \mathcal{R}^n$:

$$s(\xi, \mu) = S\xi + \mu, \quad \forall t \geq 0$$

where $S \in \mathcal{R}^{n\times 4n}$ is constant and $\text{rank}(S) = n$; $\mu : \mathcal{R}^{4n} \times \mathcal{R}_0^+ \to \mathcal{R}^n$ is a shifting factor reflecting some expected performances about the sliding surface

$$\mathcal{S}_t(\mu) = \{\xi \in \mathcal{R}^{4n} : s(\xi, \mu) = 0\}$$

Next, to explicate the sliding mode control u_r, let us introduce the following coordinates transformation to (12).

$$\left[\begin{array}{c} \xi_1 \\ \hline s(\xi, \mu) \end{array}\right] = \left[\begin{array}{c|c} I_{3n} & 0 \\ \hline S_1 & S_2 \end{array}\right] \left[\begin{array}{c} \xi_1 \\ \hline \xi_2 \end{array}\right] + \left[\begin{array}{c} 0 \\ \hline \mu \end{array}\right]$$

It follows that

$$\left[\begin{array}{c} \dot{\xi}_1 \\ \hline \dot{s}(\xi, \mu) \end{array}\right] = \left[\begin{array}{c|c} A_{11} & A_{12} \\ \hline S_1A_{11} & S_1A_{12} + S_2A_{22} \end{array}\right] \cdot \left[\begin{array}{c} \xi_1 \\ \hline \xi_2 \end{array}\right] + \left[\begin{array}{c} 0 \\ \hline S_2u_r + \dot{\mu} \end{array}\right]$$

Note that $s(\xi, \mu) = S_1\xi_1 + S_2\xi_2 + \mu$. It follows that

$$\xi_2 = S_2^{-1}[s(\xi, \mu) - \mu] - S_2^{-1}S_1\xi_1$$

This leads that

$$\left[\begin{array}{c} \dot{\xi}_1 \\ \hline \dot{s}(\xi, \mu) \end{array}\right] = \left[\begin{array}{c} \Lambda_{01} \\ \hline \Lambda_{02} \end{array}\right] + \left[\begin{array}{c} 0 \\ \hline S_2u_r + \dot{\mu} \end{array}\right]$$

where

$$\begin{cases} \Lambda_{01} = [A_{11} - A_{12}S_2^{-1}S_1]\xi_1 \\ \qquad\quad + A_{12}S_2^{-1}[s(\xi, \mu) - \mu] \\ \Lambda_{02} = [S_1A_{11} - (S_1A_{12} + S_2A_{22})S_2^{-1}S_1]\xi_1 \\ \qquad\quad + (S_1A_{12} + S_2A_{22})S_2^{-1}[s(\xi, \mu) - \mu] \end{cases}$$

In summary, the leader-average equation (12) is expressed under the new coordinates as

$$\begin{cases} \dot{\xi}_1 = \Lambda_{11}\xi_1 + \Lambda_{12}S_2^{-1}[s(\xi,\mu)-\mu] \\ \dot{s}(\xi,\mu) = S_2\Lambda_{21}\xi_1 + S_2\Lambda_{22}S_2^{-1}[s(\xi,\mu)-\mu] \\ \qquad\qquad + S_2u_r + \dot{\mu} \end{cases} \tag{13}$$

where

$$\begin{cases} \Lambda_{11} = A_{11} - A_{12}S_2^{-1}S_1 \in \mathcal{R}^{3n\times 3n} \\ \Lambda_{12} = A_{12} \in \mathcal{R}^{3n\times n} \\ \Lambda_{21} = S_2^{-1}S_1\Lambda_{11} - A_{22}S_2^{-1}S_1 \in \mathcal{R}^{n\times 3n} \\ \Lambda_{22} = S_2^{-1}S_1A_{12} + A_{22} \in \mathcal{R}^{n\times n} \end{cases}$$

Note that (A_{11}, A_{12}) is controllable. Then, we can always prescribe a non-singular $S_2 \in \mathcal{R}^{n\times n}$ and $S_1 \in \mathcal{R}^{3n\times n}$ such that all eigenvalues of $\Lambda_{11} = A_{11} - A_{12}S_2^{-1}S_1$ have negative real parts via pole assignment. The eigenvalue assignment of Λ_{11} plays a key role in ensuring that the state solution of (13) is at least ultimately bounded, which in turn guarantees that the desired sliding mode will be maintained after reaching the sliding surface [12].

C. EXISTENCE AND PROPERTIES FOR SMC

Now let us construct the sliding mode control u_r by

$$u_r = u_{r1} + u_{r2}, \quad t \geq 0 \tag{14}$$

where

$$\begin{cases} u_{r1} = -\Lambda_{21}\xi_1 - \Lambda_{22}S_2^{-1}[s(\xi,\mu)-\mu] + S_2^{-1}\Xi s(\xi,\mu) \\ u_{r2} = S_2^{-1}\Big[-\dot{\mu} - \beta\dfrac{\Upsilon s(\xi,\mu)}{||\Upsilon s(\xi,\mu)||}\Big], \quad s(\xi,\mu)\neq 0 \end{cases} \tag{15}$$

with $\Xi \in \mathcal{R}^{n\times n}$, $0 < \Upsilon^T = \Upsilon \in \mathcal{R}^{n\times n}$ being design parameter matrices and $\beta > 0$ a scalar. Also, Ξ is Hurwitz and Υ is the unique solution to the Lyapunov equation $\Xi^T\Upsilon + \Upsilon\Xi = -I_n$. It must be stressed that u_{r2} is not defined at $s(\xi,\mu) = 0$. When $s(\xi,\mu) = 0$, the state vector of (13) is located on the sliding surface, where u_r will be replaced by some equivalent control u_{re} defined soon. In addition, to ensure that the control laws in (14) and (15) are implementable, bounded-ness of ξ_1, u_{r1} and μ over $t \in [0,\infty)$ is needed. This is guaranteed by the stable eigenvalues of Λ_{11}.

As a final step for fixing u_r, we specify the shifting factor μ to be differentiable with respect to t, which is our standing assumption in the discussion. Thus, μ is bounded if ξ_1 is bounded. The latter is ensured by stability of Λ_{11}.

Now we are ready to claim existence and properties for the leader-average equation (12) to run into the sliding surface $\mathcal{S}_t(\cdot)$ and remain there under the control laws (14) and (15). The proof details for Theorem 2 are given in Appendix.

Theorem 2: Consider the leader-average equation (12). Assume that the shifting factor μ in (15) is differentiable with respect to t, and $\sup_{t\in[0,\infty)}||\mu|| < \infty$. If $S = [S_1, S_2]$ is taken such that S_2 is non-singular and all eigenvalues of $\Lambda_{11} = A_{11} - A_{12}S_2^{-1}S_1$ possess negative real parts, namely

$$\max_{i=1,\cdots,3n}\{Re(\lambda_i(\Lambda_{11}))\} < 0 \tag{16}$$

Then, the state vector of (12) will be driven into the sliding surface $\mathcal{S}_t(\mu)$ in finite time $t_s < \infty$ by the control input u_r in (14) and (15) when $s(\xi,\mu) \neq 0$, and remain there over $t \in [t_s,\infty)$ under the equivalent control

$$u_{re} = -\Lambda_{21}\xi_1 + \Lambda_{22}S_2^{-1}\mu - S_2^{-1}\dot{\mu} \tag{17}$$

when $s(\xi,\mu) = 0$.

Several remarks about Theorem 2.

- A procedure for fixing $S = [S_1, S_2]$ is: firstly, choose $K \in \mathcal{R}^{n\times 3n}$ such that all eigenvalues of $A_{11} - A_{12}K$ have negative rear parts and thus $\max\{\mathrm{Re}(\lambda(\Lambda_{11}))\}$ is fixed; secondly, take $S_1 \in \mathcal{R}^{n\times 3n}$ and nonsingular $S_2 \in \mathcal{R}^{n\times n}$ such that $S_2^{-1}S_1 = K$; thirdly, write $S_1' = \delta S_1$ and $S_2' = \delta S_2$ for some sufficiently large $\delta > 0$ as a scaling parameter so that $\max_{i=1,\cdots,3n}\{\mathrm{Re}(\lambda_i(A_{11} - A_{12}K))\} < 0$; fourthly, since $(S_2')^{-1}S_1' = S_2^{-1}S_1 = K$, all assumptions of Theorem 1 are satisfied with $S = [\delta S_1, \delta S_2]$. Clearly, some trial-and-error is needed.
- Since the sliding mode control u_r in (14), (15) contains sign operations, chattering might be brought into the flocking control algorithm (5). However, if we see that u_r is merely an indirect input to induce the desirable average trajectory in terms of q_r and p_r. It is q_r and p_r that bring the leader navigation into the the flocking control algorithm (5). Clearly, q_r and p_r themselves have no chattering, since the leader-average model acts actually as a low-passing filter.

V. MULTI-AGENT FORMATION WITH FINITE-TIME TRAJECTORY TRACKING UNDER SMC

A. PROBLEM FORMULATION AND SOLUTION

The problem is: determine possible control u_r such that in the leader-average model with the output relation (18), it is satisfied that $y = \mu$ for all $t \geq t_s$ within finite time $t_s < \infty$. Here, μ stands for the desired average trajectory.

$$\begin{cases} \begin{bmatrix} \dot{\xi}_1 \\ \dot{\xi}_2 \end{bmatrix} = \left[\begin{array}{c|c} A_{11} & A_{12} \\ \hline 0 & A_{22} \end{array}\right]\begin{bmatrix} \xi_1 \\ \xi_2 \end{bmatrix} + \begin{bmatrix} 0 \\ I_n \end{bmatrix}u_r \\ y = \underbrace{\left[\begin{array}{c|c} C_1 & C_2 \end{array}\right]}_{C}\begin{bmatrix} \xi_1 \\ \xi_2 \end{bmatrix} \end{cases} \tag{18}$$

To address the problem, let us define the switching function and sliding surface as

$$\begin{cases} s(\xi,\eta) = -C\xi + \mu \\ \mathcal{S}_t(\xi) = \{\xi \in \mathcal{R}^{4n} : -C\xi + \mu = 0\} \end{cases}$$

Then, we must answer: under what conditions does any SMC control u_r exist such that the leader-average output y will be forced to the trajectory μ (or the sliding surface $\mathcal{S}_t(\cdot)$) in finite time and remain there thereafter?

Corollary 1: In the leader-average model with the output relation in (18), assume that $C = [C_1, C_2] \in \mathcal{R}^{n\times 4n}$ with $C_2 \in \mathcal{R}^{n\times n}$ being nonsingular such that $A_{11} - A_{12}C_2^{-1}C_1$ is Hurwitz. Then, under the sliding mode control u_r in (14)

and (15) when $s(\xi,\mu)\neq 0$, the output vector of (18) will be driven to the sliding surface $\mathcal{S}_t(\xi)$ in finite time $t_s<\infty$ and thus $y=\mu$ for all $t\geq t_s$. The equivalent control for the trajectory tracking when $s(\xi,\mu)=0$ is

$$u_{re}=-\Lambda_{21}\xi_1-\Lambda_{22}C_2^{-1}\mu+C_2^{-1}\dot{\mu},\quad t\geq t_s$$

In the above, μ is the desired average trajectory.

Proof of Corollary 1: It is straightforward to show that all the conditions of Theorem 2 are satisfied. Therefore, the results follow from Theorem 2 readily. **Q.E.D**

Several remarks about Corollary 1.

- The trajectory tracking is meant in the leader-average dynamics, rather than the multi-agent ones. Main advantages of the SMC technique include: firstly, the tracking output reaches the desired trajectory in finite time; secondly, the reference tracking is totally free from matched uncertainties and robust to bounded unmatched uncertainties; thirdly, no chattering control actions involved in the flocking control.
- Different from the internal mode principle for trajectory tracking, no trajectory modeling is involved. Moreover, the multi-agent formation control laws and the control law to induce the sliding mode are designed separately.
- The finite time $t_s<\infty$ is in the sense of the output vector of the leader-average dynamics. In other words, we cannot claim any finite-time reaching to the sliding surface for the individual agents themselves in general.

B. IMPLEMENTING MULTI-AGENT FLOCKING CONTROL WITH LEADER-AVERAGE SMC

Now we consider implementation of the time-varying flocking algorithm (5) while the average dynamics are tracking a specific trajectory via SMC, which is induced by u_r defined in (14), (15) and (17) as appropriately. Since the time-varying flocking algorithm (5) consists of three terms, in which only $u_{3,i}$ is related to the leader-average dynamics in terms of q_r and p_r. In view of this, our discussion goes to how to determine q_r and p_r.

Under the assumptions of Corollary 2, when the desired trajectory μ is given, we write

$$\begin{cases}E_{11}=:-\Lambda_{21}-\Lambda_{22}C_2^{-1}C_1+C_2^{-1}\Xi C_1\\ E_{12}=:-\Lambda_{22}+C_2^{-1}\Xi C_2\\ E_{re,1}=:-\Lambda_{21}\end{cases}$$

It follows that

$$\begin{cases}u_r=E_{11}\xi_1+E_{12}\xi_2-C_2^{-1}\Xi\mu+C_2^{-1}\dot{\mu}\\ \qquad+\gamma\dfrac{C_2^{-1}\Upsilon(\mu-C\xi)}{||\Upsilon(\mu-C\xi)||},\quad \mu-C\xi\neq 0\\ u_{re}=E_{re,1}\xi_1-\Lambda_{22}C_2^{-1}\mu+C_2^{-1}\dot{\mu},\quad \mu-C\xi=0\end{cases}$$

Substituting u_r and u_{re} for the closed-loop leader-average equation, we obtain that

$$\begin{cases}\dot{\xi}=\left[\begin{array}{c|c}A_{11}&A_{12}\\ \hline E_{11}&A_{22}+E_{12}\end{array}\right]\xi+\left[\begin{array}{c}0\\ \hline I_n\end{array}\right]C_2^{-1}\\ \quad\cdot(-\Xi\mu+\dot{\mu}+\beta\dfrac{\Upsilon(\mu-C\xi)}{||\Upsilon(\mu-C\xi)||}),\\ \qquad\qquad\mu-C\xi\neq 0\\ \dot{\xi}=\left[\begin{array}{c|c}A_{11}&A_{12}\\ \hline E_{re,1}&A_{22}\end{array}\right]\xi+\left[\begin{array}{c}0\\ \hline I_n\end{array}\right]\\ \quad\cdot(-\Lambda_{22}C_2^{-1}\mu+C_2^{-1}\dot{\mu}),\quad \mu-C\xi=0\end{cases}\tag{19}$$

VI. NUMERICAL ILLUSTRATIONS

Now we sketch numerical simulations about second-order integral multi-agent networks to illustrate the main results.

Throughout the following figures, in the sub-figures captioned by (a), the dots represent the agent positions, and the arrows stand for the agent velocities; the undirected lines in between the dots reflect that the agents are within each other's γ-neighbourhood; the blue-dashed curve represents the expected trajectory, while the red-solid curve is the multi-agent average trajectory. In the sub-figures captioned by (b), the control action vectors are plotted with respect to time t in a per-dimension way.

A. TRAJECTORY-TRACKING FORMATION OF 2D MULTI-AGENT NETWORK

Consider a 2-dimensional second-order integral multi-agent network with 6 individuals. Initial position and velocity conditions of the multi-agents are randomly created within $[-10,10]\times[-10,10]$ and $[-5,5]\times[-5,5]$, respectively. The leader's initial conditions are $q_r(0)=[0;0]$, $p_r(0)=[0;0]$ and $u_r(0)=[0;0]$.

According to Corollary 2 and its implementation formulas, the algorithm parameters in (5) are: $\epsilon=0.1$, $a=5$, $b=5$, $\eta=0.6$, $d=12$, $\gamma=1.2d=14.4$, and

$$\begin{cases}\Phi=\sqrt{0.2}I_2,\quad \Psi=20I_2\\ \Xi=-0.5,\quad \beta=3\times 10^3\\ C=[-128.64,\ 0,\ -94.4,\ 0,\ 129.6,\ 0,\ 96,\ 0;\\ \qquad 0,\ -128.64,\ 0,\ -94.4,\ 0,\ 129.6,\ 0,\ 96]\end{cases}$$

In the 2-dimensional case, the trajectory $\mu=[x,y]^T$ is defined as

$$\begin{cases}x(t)=100\sin(2\pi t/100)\\ y(t)=100\cos(2\pi t/100)\end{cases}$$

More precisely, Figure 1(a) gives the multi-agent trajectory-tracking flocking in the time interval $[0,600]s$ with fixed formation determined by the constant weighting matrix $M_t=1.2I_2$. The multi-agent formations are plotted every ten seconds during the first hundred seconds and every fifty-four seconds during the other time in Figure 1(a). Figure 1(b) illustrates the control actions during $[0,100]s$, together with

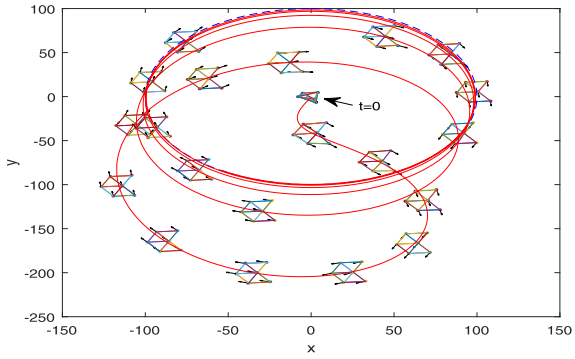

(a) fixed formation with $M_t = 1.2I_2$

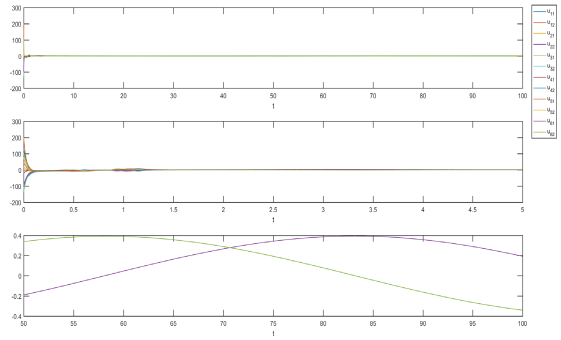

(b) control actions under $M_t = 1.2I_2$

FIGURE 1. Fixed trajectory-tracking formation with SMC in the 2D case.

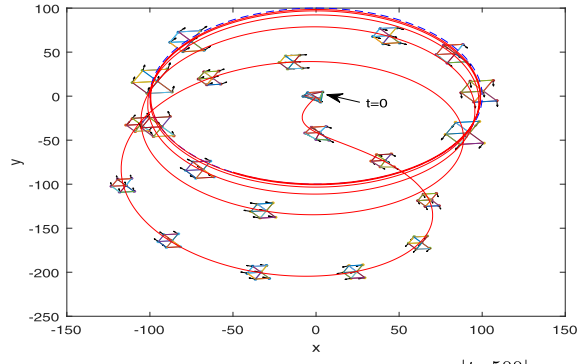

(a) flexible formation with $M_t = (1 + \frac{|t-500|}{500})I_2$

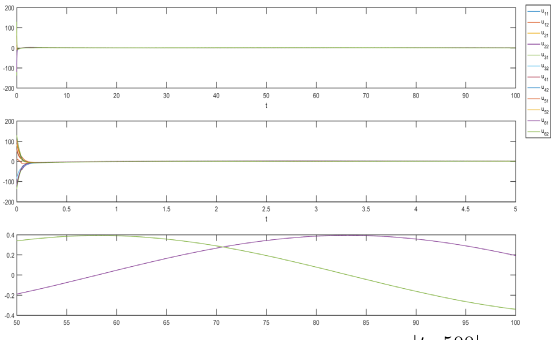

(b) control actions under $M_t = (1 + \frac{|t-500|}{500})I_2$

FIGURE 2. Flexible trajectory-tracking formation with SMC in the 2D case.

those over $[0, 5]s$ and $[50, 100]s$. It is worth noticing that no control action chattering is involved.

Figure 2 presents the results under the time-varying weighting matrix $M_t = (1 + \frac{|t-500|}{500})I_2$. In particular,

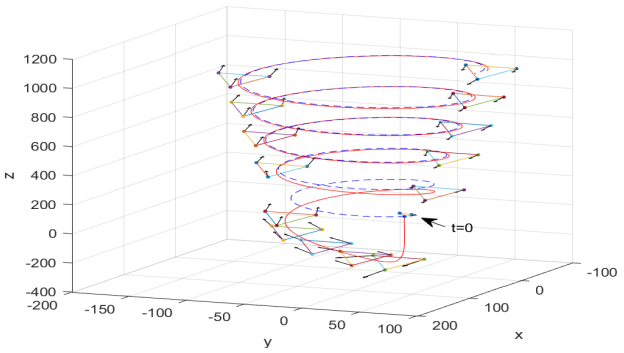

(a) fixed formation with $M_t = 1.2I_3$

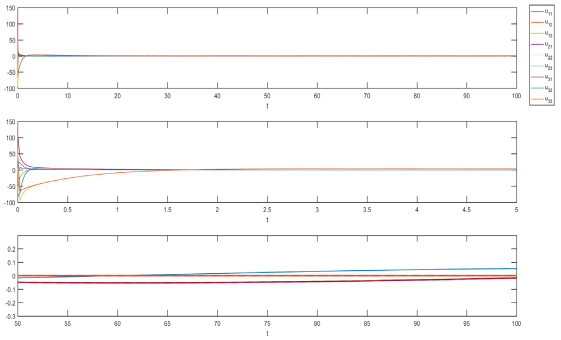

(b) control actions under $M_t = 1.2I_3$

FIGURE 3. Fixed trajectory-tracking multi-agent formation with SMC in the 3D case.

when $||M_t||$ decreases during $t \in [0, 500)$, then the formation scales up gradually; when $||M_t||$ is increasing during $t \in [500, 600)$, then the formation scales down gradually. This reveals that the formation scaling can be adjusted by choosing the weighting matrix M_t as appropriately.

Clearly, in both cases the desired multi-agent formation is yielded, and the formation average position runs into the expected trajectory.

B. TRAJECTORY-TRACKING FORMATION OF 3D MULTI-AGENT NETWORK

Consider a 3-dimensional multi-agent integral network with 3 individuals. Initial position and velocity conditions of the multi-agents are randomly created within $[-10, 10] \times [-10, 10] \times [-10, 10]$ and $[-5, 5] \times [-5, 5] \times [-5, 5]$, respectively. The leader's initial conditions are $q_r(0) = [0; 0; 0]$, $p_r(0) = [0; 0; 0]$ and $u_r(0) = [0; 0; 0]$.

According to Corollary 2 and its implementation formulas, the algorithm parameters in (5) are: $\epsilon = 0.1$, $a = 5$, $b = 5$, $\eta = 0.6$, $d = 60$, $\gamma = 1.2d = 72$, and

$$\begin{cases} \Phi = \sqrt{0.2}I_3, \quad \Psi = 20I_3 \\ \Xi = -0.5, \quad \beta = 3 \times 10^3 \\ C = [-135.474,\ 0,\ 0,\ -99.415,\ 0,\ 0,\ 136.485,\ 0,\ 0, \\ \qquad 101.1,\ 0,\ 0;\ 0,\ -135.474,\ 0,\ 0,\ -99.415,\ 0,\ 0, \\ \qquad 136.485,\ 0,\ 0,\ 101.1,\ 0;\ 0,\ 0,\ -135.474,\ 0,\ 0, \\ \qquad -99.415,\ 0,\ 0,\ 136.485,\ 0,\ 0,\ 101.1] \end{cases}$$

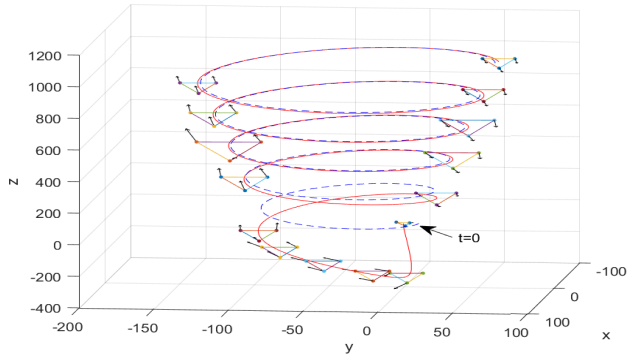

(a) flexible formation with $M_t = (1 + \frac{|t-500|}{500})I_3$

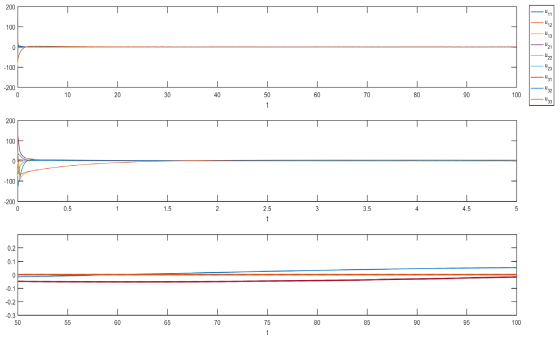

(b) control actions under $M_t = (1 + \frac{|t-500|}{500})I_3$

FIGURE 4. Flexible trajectory-tracking multi-agent formation with SMC in the 3D case.

In the 3-dimensional case, the trajectory $\mu = [x, y, z]^T$ is given by

$$\begin{cases} x(t) = (10 + 0.1t)\sin(2\pi t/200) \\ y(t) = (10 + 0.1t)\cos(2\pi t/200) - 40 \\ z(t) = t \end{cases}$$

which is illustrated with the blue-dashed curve.

More precisely, Figure 3(a) gives the multi-agent trajectory-tracking flocking with a fixed formation determined by the constant weighting matrix $M_t = 1.2I_3$ during the time interval $[0, 1000]s$. The multi-agent formations are plotted every twenty seconds during the first two hundred seconds and every hundred seconds during the other time in Figure 3(a). Figure 3(b) illustrates the control actions during $[0, 100]s$, together with those over $[0, 5]s$ and $[50, 100]s$, in which no control action chattering can be seen.

Figure 4(a) illustrates the results with a flexible formation determined by the time-varying weighting matrix $M_t = (1 + \frac{|t-500|}{500})I_3$. Similar to the 2D case, when $||M_t||$ decreases with respect to $t \in [0, 500)$, the formation scales up gradually; when $||M_t||$ increases with respect to $t \in [500, 1000)$, the formation scales down gradually.

Obviously, in both cases the desired formation is yielded, and the average position runs into the specified trajectory.

VII. CONCLUSION

This paper is devoted to trajectory-tracking flexible formation control of second-order integral multi-agent networks with single virtual leaders. In other words, the Olfati-Saber's flocking algorithms are modified into a class of generalized ones with time-varying weighting parameters; then trajectory-tracking control is worked out with sliding mode control in the sense of the leader-average dynamics. This technique provides us with more design freedoms for dealing with multi-objectives and performances. General time-varying multi-agent formation existence and properties are summarized in Theorem 1, whereas SMC-specifying trajectory-tracking formation design is explained by Theorem 2 and Corollary 1, whose implementation is also summarized. The proposed SMC-specification approach is inspiring and meaningful for other multi-agent control issues such as collision avoidance and route planning.

APPENDIX

PROOF OF THEOREM 2

The proof arguments are completed in two steps.

Step 1: It is shown that the state vector of (12) can be driven into the sliding surface $\mathcal{S}_t(\mu)$ in finite time $t_s < \infty$.

To this end, we construct the Lyapunov function $V(s) = \frac{1}{2}s^T(\xi, \mu)\Upsilon s(\xi, \mu)$. When $s(\xi, \mu) \neq 0$ (that is, the concerned state vector has not reached the sliding surface), its derivative with respect to t ($t \geq 0$) along (13) can be given by

$$\begin{aligned}
\dot{V}(s) &= s^T(\xi, \mu)\Upsilon\dot{s}(\xi, \mu) \\
&= s^T(\xi, \mu)\Upsilon\Big(S_2\Lambda_{21}\xi_1 \\
&\quad + S_2\Lambda_{22}S_2^{-1}[s(\xi, \mu) - \mu] + S_2u_r + \dot{\mu}\Big) \\
&= s^T(\xi, \mu)\Upsilon\Big(S_2\Lambda_{21}\xi_1 + S_2\Lambda_{22}S_2^{-1}[s(\xi, \mu) - \mu] \\
&\quad + \dot{\mu} + S_2\Big[S_2^{-1}[-S_2\Lambda_{21}\xi_1 - S_2\Lambda_{22}S_2^{-1} \\
&\quad \cdot [s(\xi, \mu) - \mu] + \Xi s(\xi, \mu)]\Big] \\
&\quad + S_2\Big[S_2^{-1}[-\dot{\mu} - \beta\frac{\Upsilon s(\xi, \mu)}{||\Upsilon s(\xi, \mu)||}]\Big]\Big) \\
&= s^T(\xi, \mu)\Upsilon\Xi s(\xi, \mu) - \beta s^T(\xi, \mu)\frac{\Upsilon^2 s(\xi, \mu)}{||\Upsilon s(\xi, \mu)||} \\
&= -\frac{1}{2}s^T(\xi, \mu)s(\xi, \mu) - \beta s^T(\xi, \mu)\frac{\Upsilon^2 s(\xi, \mu)}{||\Upsilon s(\xi, \mu)||} \\
&= -\frac{1}{2}s^T(\xi, \mu)s(\xi, \mu) - \beta||\Upsilon s(\xi, \mu)|| \\
&\leq -\frac{1}{2}s^T(\xi, \mu)s(\xi, \mu) - \beta\sqrt{2\lambda_{\min}(\Upsilon)V(s)}
\end{aligned}$$

where the Rayleigh quotient principle (Lemma 8.4.3 [2, p. 467]) and $\Upsilon = Z^TZ = ZZ^T$ for some square-root matrix $Z^T = Z \in \mathcal{R}^{n\times n}$ are used. Indeed, we have

$$\begin{aligned}
||\Upsilon s(\xi, \mu)||^2 &= s^T(\xi, \mu)\Upsilon^T\Upsilon s(\xi, \mu) \\
&= (Zs(\xi, \mu))^T(ZZ^T)(Zs(\xi, \mu)) \\
&= (Zs(\xi, \mu))^T\Upsilon(Zs(\xi, \mu)) \\
&\geq \lambda_{\min}(\Upsilon)(Zs^T(\xi, \mu))^T(Zs(\xi, \mu)) \\
&= \lambda_{\min}(\Upsilon)s^T(\xi, \mu)Z^TZs(\xi, \mu)) \\
&= 2\lambda_{\min}(\Upsilon)V(s)
\end{aligned}$$

The arguments, with $s^T(\xi,\mu)s(\xi,\mu)\geq 0$, lead that

$$\dot{V}(s)\leq -\beta\sqrt{2\lambda_{\min}(\Upsilon)V(s)}$$

Integrating the above inequality in time implies that the time for the system dynamics to reach the sliding surface $\mathcal{S}_t(\mu)$, denoted by t_s, must satisfy

$$t_s\leq \beta^{-1}\sqrt{2\,V(s_0)/\lambda_{\min}(\Upsilon)}$$

where s_0 denotes the initial value of $s(\xi,\mu)$ at $t=0$.

Step 2: It is shown that the state vector remains on the sliding surface thereafter if some implementable control u_r over $t\in[t_s,\infty)$ exists.

Clearly, when the state vector reaches the sliding surface and remains there, it holds that $s(\xi,\mu)=0$ over $t\in[t_s,\infty)$. This is equivalent to saying that the leader-average dynamics reduce to the following.

$$\begin{cases}\dot{\xi}_1=\Lambda_{11}\xi_1-\Lambda_{12}S_2^{-1}\mu\\ \dot{s}(\xi,\mu)=S_2\Lambda_{21}\xi_1-S_2\Lambda_{22}S_2^{-1}\mu+S_2u_r+\dot{\mu}\\ t\in[t_s,\infty)\end{cases}\tag{20}$$

For the state vector remains on the sliding surface over $t\in[t_s,\infty)$, it is necessary to choose u_r such that $\dot{s}(\xi,\mu)=0$ over $t\in[t_s,\infty)$. The corresponding u_r is called the equivalent control, denoted by u_{re} hereafter and given as in (17).

After reaching the sliding surface, if the control u_r is replaced with u_{re} of (17), then the state vector remains on the sliding surface, whenever u_{re} is implementable in the sense that ξ_1, μ and $\dot{\mu}$ are all bounded. To this end, let $0<\Upsilon'=\Upsilon'^T\in\mathcal{R}^{3n\times 3n}$ be the unique solution to the algebraic Lyapunov equation $\Lambda_{11}^T\Upsilon'+\Upsilon'\Lambda_{11}=-Q$ with $0<Q=Q^T\in\mathcal{R}^{3n\times 3n}$. Consider the Lyapunov candidate $V(\xi_1)=\frac{1}{2}\xi_1^T\Upsilon'\xi_1$ for the first equation of (20). Then, the time derivative of $V(\xi_1)$ along the first equation of (20) gives

$$\begin{aligned}\dot{V}(\xi_1)&=\xi_1^T\Upsilon'\dot{\xi}_1=\xi_1^T\Upsilon'[\Lambda_{11}\xi_1-\Lambda_{12}S_2^{-1}\mu]\\&=\xi_1^T\Upsilon'\Lambda_{11}\xi_1-\xi_1^T\Upsilon'\Lambda_{12}S_2^{-1}\mu\\&=-\frac{1}{2}\xi_1^TQ\xi_1-\xi_1^T\Upsilon'\Lambda_{12}S_2^{-1}\mu\\&\leq-\frac{1}{2}\xi_1^TQ\xi_1+||\Upsilon'\Lambda_{12}S_2^{-1}\xi_1||\cdot||\mu||\\&\leq-\frac{1}{2}\lambda_{\min}(Q)\cdot||\xi_1||^2\\&\quad+\lambda_{\max}(\Upsilon')||\Lambda_{12}S_2^{-1}\xi_1||\cdot||\mu||\\&\leq-\frac{1}{2}\lambda_{\min}(Q)\cdot||\xi_1||^2\\&\quad+\lambda_{\max}(\Upsilon')||\Lambda_{12}S_2^{-1}||\cdot||\xi_1||\cdot||\mu||\\&=-||\xi_1||\Big[\frac{1}{2}\lambda_{\min}(Q)\cdot||\xi_1||\\&\quad-\lambda_{\max}(\Upsilon')||\Lambda_{12}S_2^{-1}||\cdot||\mu||\Big]\\&=-||\xi_1||\Big(\lambda_{\max}(\Upsilon')||\Lambda_{12}S_2^{-1}||\Big)\\&\quad\cdot\Big[K||\xi_1||-||\mu||\Big]\end{aligned}\tag{21}$$

where $t\in[t_s,\infty)$ and we simply write

$$K=\frac{\lambda_{\min}(Q)}{2\lambda_{\max}(\Upsilon')||\Lambda_{12}S_2^{-1}||}$$

The inequalities in (21) say that if

$$K||\xi_1||>||\mu||,\quad t\in[t_s,\infty)\tag{22}$$

then $\dot{V}(\xi_1)<0$ over $t\in[t_s,\infty)$ and thus the solutions to the first equation of (20) are at least bounded. Bearing in mind the above inequality, we see that if

$$K||\xi_1||>\sup_{t\geq 0}||\mu||\tag{23}$$

holds true, then the inequality (22) is true. To see under what conditions about μ the inequality (23) can be ensured, we consider two situations: $\mu=0$ and $\mu\neq 0$.

On the one hand, when $\mu=0$, the inequality (22) holds in form of

$$K>0,\quad\forall\xi_1\in\mathcal{R}^{3n}\tag{24}$$

This is always possible by choosing S_2. Indeed, in this situation the solution $\xi=[\xi_1^T,\xi_2^T]^T$ is actually asymptotically stable, and thus ultimately bounded.

On the other hand, when $\mu\neq 0$ and $\sup_{t\geq 0}||\mu||>0$, it is not possible to claim asymptotical stability; actually no inequality independent of $||\xi_1||$ can be derived from (23). To surmount this problem, let us return to the last inequality of (21) and observe that

$$\dot{V}(\xi_1)\leq-||\xi_1||\Big(\lambda_{\max}(\Upsilon')||\Lambda_{12}S_2^{-1}||\Big)\cdot\Big[K||\xi_1||-\sup_{t\geq 0}||\mu||\Big]$$

Without loss of generality, let us assume that $K>0$. It follows that $\dot{V}(\xi_1)<0$ if

$$||\xi_1||>\sup_{t\geq 0}||\mu||/K$$

Hence, for any ξ_1 that does not satisfy the above inequality, it will evolve into the set ultimately. Namely, $\xi=[\xi_1^T,\xi_2^T]^T$ is ultimately bounded when $\mu\neq 0$.

In short, if (24) holds, then the solution $\xi=[\xi_1^T,\xi_2^T]^T$ is at least ultimately bounded so that the equivalent control u_{re} is implementable; or equivalently, the state vector is kept on the sliding surface by $u_r=u_{re}$ for all $t\geq t_s$.

To complete the proof in Step 2, let us note that (24) can be re-written as

$$\frac{\lambda_{\min}(Q)}{2\lambda_{\max}(\Upsilon')||\Lambda_{12}S_2^{-1}||}>0$$

Now we consider the optimal choice of Q to maximize $\lambda_{\min}(Q)/\lambda_{\max}(\Upsilon')$. The optimal solution is given as follows when $Q=I_{3n}$.

$$\begin{aligned}\max\{\lambda_{\min}(Q)/\lambda_{\max}(\Upsilon')\}&=1/\lambda_{\max}(\Upsilon')\\&\leq-2\max\{\mathrm{Re}\lambda(\Lambda_{11})\}\end{aligned}$$

Then, it follows that (24) holds true if

$$\frac{-2\max\{\mathrm{Re}\lambda(\Lambda_{11})\}}{2||\Lambda_{12}S_2^{-1}||}>0$$

which yields (16), noting that $\Lambda_{11} = A_{11} - A_{12}S_2^{-1}S_1$ and $\Lambda_{12} = A_{12}$.

REFERENCES

[1] L. Brinon-Arranz, A. Seuret, and C. Canudas-de-Wit, "Cooperative control design for time-varying formations of multi-agent systems," *IEEE Trans. Autom. Control*, vol. 59, no. 8, pp. 2283–2288, Aug. 2014.

[2] D. S. Bernstein, *Matrix Mathematics: Theory, Facts, and Formulas*, 2nd ed. Princeton, NJ, USA: Princeton Univ. Press, 2009.

[3] A. N. Bishop, M. Deghat, B. D. O. Anderson, and Y. Hong, "Distributed formation control with relaxed motion requirements," *Int. J. Robust Nonlinear Control*, vol. 25, no. 17, pp. 3210–3230, Oct. 2014.

[4] X. Bu, L. Cui, Z. Hou, and W. Qian, "Formation control for a class of nonlinear multiagent systems using model-free adaptive iterative learning," *Int. J. Robust Nonlinear Control*, vol. 28, no. 4, pp. 1402–1412, Oct. 2017.

[5] X. Chen and F. Hao, "Event-triggered average consensus control for discrete-time multi-agent systems," *IET Control Theory Appl.*, vol. 6, no. 16, pp. 2493–2498, Nov. 2012.

[6] M. L. Corradini and G. Orlando, "Variable structure control of discretized continuous-time systems," *IEEE Trans. Autom. Control*, vol. 43, no. 9, pp. 1329–1334, Sep. 1998.

[7] M. Deghat, B. D. O. Anderson, and Z. Lin, "Combined flocking and distance-based shape control of multi-agent formations," *IEEE Trans. Autom. Control*, vol. 61, no. 7, pp. 1824–1837, Jul. 2016.

[8] X. Dong, Q. Li, Z. Ren, and Y. Zhong, "Formation-containment control for high-order linear time-invariant multi-agent systems with time delays," *J. Franklin Inst.*, vol. 352, no. 9, pp. 3564–3584, Sep. 2015.

[9] X. Dong and G. Hu, "Time-varying formation control for general linear multi-agent systems with switching directed topologies," *Automatica*, vol. 73, pp. 47–55, Nov. 2016.

[10] X. Dong and G. Hu, "Time-varying formation tracking for linear multiagent systems with multiple leaders," *IEEE Trans. Autom. Control*, vol. 62, no. 7, pp. 3658–3664, Jul. 2017.

[11] H. Du, S. Li, and X. Lin, "Finite-time formation control of multiagent systems via dynamic output feedback," *Int. J. Robust Nonlinear Control*, vol. 23, no. 14, pp. 1609–1628, Jun. 2012.

[12] C. Edwards and S. K. Spurgeon, *Sliding Mode Control-Theory and Applications*. New York, NY, USA: Taylor & Francis, 1998.

[13] Y. Gao, L. Wang, G. Xie, and B. Wu, "Consensus of multi-agent systems based on sampled-data control," *Int. J. Control*, vol. 82, no. 12, pp. 2193–2205, Oct. 2009.

[14] W. N. Gao, Z. P. Jiang, F. L. Lewis, and Y. B. Wang, "Leader-to-formation stability of multiagent systems: An adaptive optimal control approach," *IEEE Trans. Autom. Control*, vol. 63, no. 10, pp. 3581–3587, Oct. 2018.

[15] Q. Gong, C. Wang, Z. Qi, and Z. Ding, "Gradient-based collision avoidance algorithm for second-order multi-agent formation control," in *Proc. 36th Chin. Control Conf. (CCC)*, Dalian, China, Jul. 2017, pp. 8183–8188.

[16] T.-T. Han and S. S. Ge, "Styled-velocity flocking of autonomous vehicles: A systematic design," *IEEE Trans. Autom. Control*, vol. 60, no. 8, pp. 2015–2030, Aug. 2015.

[17] L. S. Hu, T. Bai, P. Shi, and Z. M. Wu, "Sampled-data control of networked linear control systems," *Automatica*, vol. 43, pp. 903–911, May 2007.

[18] A. Jadbabaie, J. Lin, and A. S. Morse, "Coordination of groups of mobile autonomous agents using nearest neighbor rules," *IEEE Trans. Autom. Control*, vol. 48, no. 6, pp. 988–1001, Jun. 2003.

[19] B. Jiang, M. Deghat, and B. D. O. Anderson, "Simultaneous velocity and position estimation via distance-only measurements with application to multi-agent system control," *IEEE Trans. Autom. Control*, vol. 62, no. 2, pp. 869–875, Feb. 2017.

[20] S.-M. Kang and H.-S. Ahn, "Shape and orientation control of moving formation in multi-agent systems without global reference frame," *Automatica*, vol. 92, pp. 210–216, Jun. 2018.

[21] H. Li, X. Liao, T. Huang, and W. Zhu, "Event-triggering sampling based leader-following consensus in second-order multi-agent systems," *IEEE Trans. Autom. Control*, vol. 60, no. 7, pp. 1998–2003, Jul. 2015.

[22] W. Li and G. Chen, "The designated convergence rate problem of consensus or flocking of double-integrator agents with general non-equal velocity and position couplings," *IEEE Trans. Autom. Control*, vol. 62, no. 1, pp. 412–418, Jan. 2017.

[23] D. Li, S. S. Ge, W. He, G. Ma, and L. Xie, "Multilayer formation control of multi-agent systems," *Automatica*, vol. 109, Nov. 2019, Art. no. 108558, doi: 10.1016/j.automatica.2019.108558.

[24] X. Li and L. Xi, "Dynamic formation control over directed networks using graphical Laplacian approach," *IEEE Trans. Autom. Control*, vol. 63, no. 11, pp. 3761–3774, Nov. 2018.

[25] Z. Lin, L. Wang, Z. Han, and M. Fu, "Distributed formation control of multi-agent systems using complex laplacian," *IEEE Trans. Autom. Control*, vol. 59, no. 7, pp. 1765–1777, Jul. 2014.

[26] L. Liu, C. Luo, and F. Shen, "Multi-agent formation control with target tracking and navigation," in *Proc. IEEE Int. Conf. Inf. Autom. (ICIA)*, Macau, China, Jul. 2017, pp. 98–103.

[27] D. Meng and Y. Jia, "Formation control for multi-agent systems through an iterative learning design approach," *Int. J. Robust Nonlinear Control*, vol. 24, no. 2, pp. 340–361, Aug. 2012.

[28] D. Meng, Y. Jia, J. Du, and J. Zhang, "On iterative learning algorithms for the formation control of nonlinear multi-agent systems," *Automatica*, vol. 50, no. 1, pp. 291–295, Jan. 2014.

[29] T. Motoyama and K. Cai, "Top-down synthesis of multiagent formation control: An eigenstructure assignment based approach," *IEEE Trans. Control Netw. Syst.*, vol. 6, no. 4, pp. 1404–1414, Dec. 2019.

[30] R. Olfati-Saber and R. M. Murray, "Consensus problems in networks of agents with switching topology and time-delays," *IEEE Trans. Autom. Control*, vol. 49, no. 9, pp. 1520–1533, Sep. 2004.

[31] R. Olfati-Saber, "Flocking for multi-agent dynamic systems: Algorithms and theory," *IEEE Trans. Autom. Control*, vol. 51, no. 3, pp. 401–420, Mar. 2006.

[32] C. Peng and Q.-L. Han, "On designing a novel self-triggered sampling scheme for networked control systems with data losses and communication delays," *IEEE Trans. Ind. Electron.*, vol. 63, no. 2, pp. 1239–1248, Feb. 2016.

[33] J. Qin, G. Zhang, W. X. Zheng, and Y. Kang, "Adaptive sliding mode consensus tracking for second-order nonlinear multiagent systems with actuator faults," *IEEE Trans. Cybern.*, vol. 49, no. 5, pp. 1605–1615, May 2019.

[34] W. Qin, Z. Liu, and Z. Chen, "Formation control for nonlinear multi-agent systems with linear extended state observer," *IEEE/CAA J. Automatica Sinica*, vol. 1, no. 2, pp. 171–179, Apr. 2014.

[35] G. S. Seyboth, W. Ren, and F. Allgöwer, "Cooperative control of linear multi-agent systems via distributed output regulation and transient synchronization," *Automatica*, vol. 68, pp. 132–139, Jun. 2016.

[36] J. J. E. Slotine and S. S. Sastry, "Tracking control of nonlinear systems using sliding surfaces with application to robot manipulators," *Int. J. Control*, vol. 38, no. 2, pp. 465–492, 1983.

[37] S. K. Spurgeon, "Hyperplane design techniques for discrete-time variable structure control systems," *Int. J. Control*, vol. 55, no. 2, pp. 445–456, Feb. 1992.

[38] H. Su, X. Wang, and W. Yang, "Flocking in multi-agent systems with multiple virtual leaders," *Asian J. Control*, vol. 10, no. 2, pp. 238–245, 2008.

[39] H. Su and G.-Y. Tang, "Rolling optimization formation control for multi-agent systems under unknown prior desired shapes," *Inf. Sci.*, vol. 459, pp. 255–264, Aug. 2018.

[40] X. Sun, Y. Peng, Q. Yin, and X. Liu, "Multi-agent formation control based on artificial force with exponential form," in *Proc. 11th World Congr. Intell. Control Autom.*, Shenyang, China, Jun. 2014, pp. 3128–3133.

[41] X. Sun and C. G. Cassandras, "Optimal dynamic formation control of multi-agent systems in constrained environments," *Automatica*, vol. 73, pp. 169–179, Nov. 2016.

[42] H. G. Tanner, A. Jadbabaie, and G. J. Pappus, "Stable flocking of mobile agents Part II: Dynamical topology," in *Proc. 42nd IEEE Conf. Decis. Control*, Dec. 2003, pp. 2016–2021.

[43] H. G. Tanner, A. Jadbabaie, and G. J. Pappas, "Flocking in fixed and switching networks," *IEEE Trans. Autom. Control*, vol. 52, no. 5, pp. 863–868, May 2007.

[44] A. Tesfaye and M. Tomizuka, "Robust control of discretized continuous systems using the theory of sliding modes," *Int. J. Control*, vol. 62, no. 1, pp. 209–226, Feb. 2007.

[45] J. Toner and Y. Tu, "Flocks, herds, and schools: A quantitative theory of flocking," *Phys. Rev. E, Stat. Phys. Plasmas Fluids Relat. Interdiscip. Top.*, vol. 58, no. 4, pp. 4828–4858, Oct. 1998.

[46] C. M. Topaz and A. L. Bertozzi, "Swarming patterns in a two-dimensional kinematic model for biological groups," *SIAM J. Appl. Math.*, vol. 65, no. 1, pp. 152–174, Jan. 2004.

[47] M. H. Trinh, S. Zhao, Z. Sun, D. Zelazo, B. D. O. Anderson, and H.-S. Ahn, "Bearing-based formation control of a group of agents with leader-first follower structure," *IEEE Trans. Autom. Control*, vol. 64, no. 2, pp. 598–613, Feb. 2019.
[48] D. Viegas, P. Batista, P. Oliveira, C. Silvestre, and C. L. P. Chen, "Distributed state estimation for linear multi-agent systems with time-varying measurement topology," *Automatica*, vol. 54, pp. 72–79, Apr. 2015.
[49] X. F. Wang and M. D. Lemmon, "Event-triggering in distriuted networked control systems," *IEEE Trans. Autom. Control*, vol. 56, no. 3, pp. 586–601, Mar. 2011.
[50] W. Rui, D. Xiwang, L. Qingdong, Z. Qilun, and R. Zhang, "Adaptive time-varying formation control for high-order LTI multi-agent systems," in *Proc. 34th Chin. Control Conf. (CCC)*, Hangzhou, China, Jul. 2015, pp. 6998–7003.
[51] C. Wang, J. Zhou, and Z. Duan, "Multi-agent collision approach for stabilizing multi-machine power networks with distributed excitation systems," *IFAC J. Syst. Control*, vol. 5, pp. 11–21, Sep. 2018.
[52] K. Xu and L. Qin, "Multi-agent formation control based on virtual forces," in *Proc. 5th Int. Conf. Inf. Sci. Technol. (ICIST)*, Changsha, China, Apr. 2015, pp. 284–291.
[53] D. Xue, J. Yao, J. Wang, Y. Guo, and X. Han, "Formation control of multi-agent systems with stochastic switching topology and time-varying communication delays," *IET Control Theory Appl.*, vol. 7, no. 13, pp. 1689–1698, Sep. 2013.
[54] D. Yang, X. Liu, and W. Chen, "Periodic event/self-triggered consensus for general continuous-time linear multi-agent systems under general directed graphs," *IET Control Theory Appl.*, vol. 9, no. 3, pp. 428–440, Feb. 2015.
[55] W. Yu, G. Chen, and M. Cao, "Distributed leader–follower flocking control for multi-agent dynamical systems with time-varying velocities," *Syst. Control Lett.*, vol. 59, no. 9, pp. 543–552, Sep. 2010.
[56] S. Yu and X. Long, "Finite-time consensus for second-order multi-agent systems with disturbances by integral sliding mode," *Automatica*, vol. 54, pp. 158–165, Apr. 2015.
[57] M. M. Zavlanos, A. Jadbabaie, and G. J. Pappas, "Flocking while preserving network connectivity," in *Proc. 46th IEEE Conf. Decis. Control*, Dec. 2007, pp. 2919–2924.
[58] B. Zheng and X. Mu, "Formation-containment control of second-order multi-agent systems with only sampled position data," *Int. J. Syst. Sci.*, vol. 47, no. 15, pp. 3609–3618, Nov. 2015.
[59] J. Zhou, C. Wang, and H. M. Qian, "Existence, properties and trajectory specification of generalised multi-agent flocking," *Int. J. Control*, vol. 92, no. 6, pp. 1434–1456, Nov. 2017.
[60] J. Zhou, X. Li, and H. Huang, "Manifold consensus of multi-machine power networks by augmented multi-agent collision control and distributed implementation," *Int. J. Control*, Aug. 2019, doi: 10.1080/00207179.2019.1652766.
[61] J. Zhou and T. Hagiwara, "Existence conditions and applications of shifting sliding mode control," in *Proc. 40th IEEE Conf. Decis. Control*, Orlando, Florida, USA, Dec. 2001, pp. 1415–1420.

JUN ZHOU (Member, IEEE) received the B.S. degree from Sichuan University, China, in 1984, the M.S. degree from Lanzhou University, China, in 1987, and the Ph.D. degree from Kyoto University, Japan, in 2002. He is currently a Professor with the Department of Control Engineering, School of Energy and Electrical Engineering, Hohai University, China. His research interests include nonlinear/hybrid systems and control, robustness performance synthesis, neural networks and learning control, multiagent and distributed sensor networks, stabilization of multimachine power systems, and periodic systems and control via harmonic analysis.

DEBIN ZENG received the B.Eng. degree from the Department of Control Engineering, School of Energy and Electrical Engineering, Hohai University, Nanjing, China, in 2019, where he is currently pursuing the master's degree. His research interests include multiagent system formation and learning control.

XINBIAO LU received the B.E. degree in metallic materials engineering from Shandong University, China, in 1998, and the M.S. and Ph.D. degrees in control theory and control engineering from Shanghai Jiao Tong University, China, in 2004 and 2008, respectively. He is currently an Associate Professor with the Department of Control Engineering, School of Energy and Electrical Engineering, Hohai University, China. His research interests include but not limited to multiagent and distributed sensor networks, and pinning control.